



Bulletin of the Mineral Research and Exploration

<http://bulletin.mta.gov.tr>



Estimating the recurrence of earthquakes with statistical methods in the city of Bingöl, Eastern Türkiye: a district-based approach

Sadık ALASHAN^{a,b,*}, Kenan AKBAYRAM^{a,b} and Ömer Faruk NEMUTLU^{a,b}

^aBingöl University, Centre for Energy, Environment and Natural Disasters, 12000 Bingöl, Türkiye.

^bBingöl University, Department of Civil Engineering, Bingöl University, 12000 Bingöl, Türkiye.

Research Article

Keywords:

Bingöl, Earthquake Magnitude, Risk, Probability Functions, Karlıova Triple Junction.

ABSTRACT

This study discusses the temporal distribution of earthquake magnitudes in the city of Bingöl, near Karlıova Triple Junction. We determine the probability distributions and return periods of earthquakes for all districts of Bingöl. Bingöl has eight districts; namely Adaklı, Central, Genç, Karlıova, Kiğı, Solhan, Yayladere, and Yedisu. In six of them, active faults were mapped previously (Adaklı, Central, Genç, Karlıova, Solhan, and Yedisu). We consider 5 time-dependent probability distributions for analysis. Using the annual maximum earthquake magnitudes, the best fit arises from the Gumbel distribution for Central, Karlıova, and Adaklı Districts. For the Genç District, where the least maximum earthquake magnitude is reported, the Weibull distribution gives the best fit. The return period and maximum annual earthquake magnitude relations suggest the following results. For the Central and Karlıova Districts along which maximum earthquake magnitudes are reported, every 250 years a 6.7 M, and 7.2 M occurs respectively. These results are compatible with the results of paleo-seismological data reported along the NAFZ and the EAFZ. For a 10-year return period, earthquake magnitudes reach 3.9 and 5.1 in all districts. It is important to note that in the Yedisu District, the maximum earthquake magnitudes seem as 5.1 M for the 1000-year return period, incompatible with previously published findings probably because of low quality seismic data in this region.

Received Date: 25.02.2022

Accepted Date: 19.01.2023

1. Introduction

Three major strike-slip fault zones of Eastern Mediterranean, the North Anatolian Fault Zone (NAFZ), the East Anatolian Fault Zone (EAFZ), and the Varto Fault Zone (VFZ), intersect at the Karlıova Triple Junction (KTJ) in the city of Bingöl, eastern Türkiye (Figure 1). The Bitlis-Zagros Active Thrust Zone (BZATZ), the tectonic boundary between the Eastern Turkish High Plateau and the Arabian Plate (Şengör, 1980), is also very close to Bingöl. Some of the active faults at the eastern end of the V-shaped area between the NAFZ and the EAFZ (e.g., Sudüğünü Fault, Sancak-Uzunpınar Fault Zone) are located in

Bingöl (Figure 1b). Many devastating earthquakes, whose historical records date back to the 10th century, were reported in this region (Ambraseys, 1989, 1970; Ambraseys and Jackson, 1998; Köküm and Özçelik, 2020). This is supported by several intense earthquakes in Bingöl and its vicinity during the instrumental period (Table 1).

Although it is impossible to determine an exact date for an expected earthquake, the probable occurrence of earthquakes can be determined with a certain margin of error. Probability distribution functions play a strong role in determining earthquake risks. The statistical modelling of earthquakes is a method

Citation Info: Alashan, S., Akbayram, K., Nemutlu, Ö. F. 2023. Estimating the recurrence of earthquakes with statistical methods in the city of Bingöl, Eastern Turkey: a district-based approach. Bulletin of the Mineral Research and Exploration 172, 15-29. <https://doi.org/10.19111/bulletinofmre.1239185>

*Corresponding author: Sadık ALASHAN, sadikalashan@bingol.edu.tr

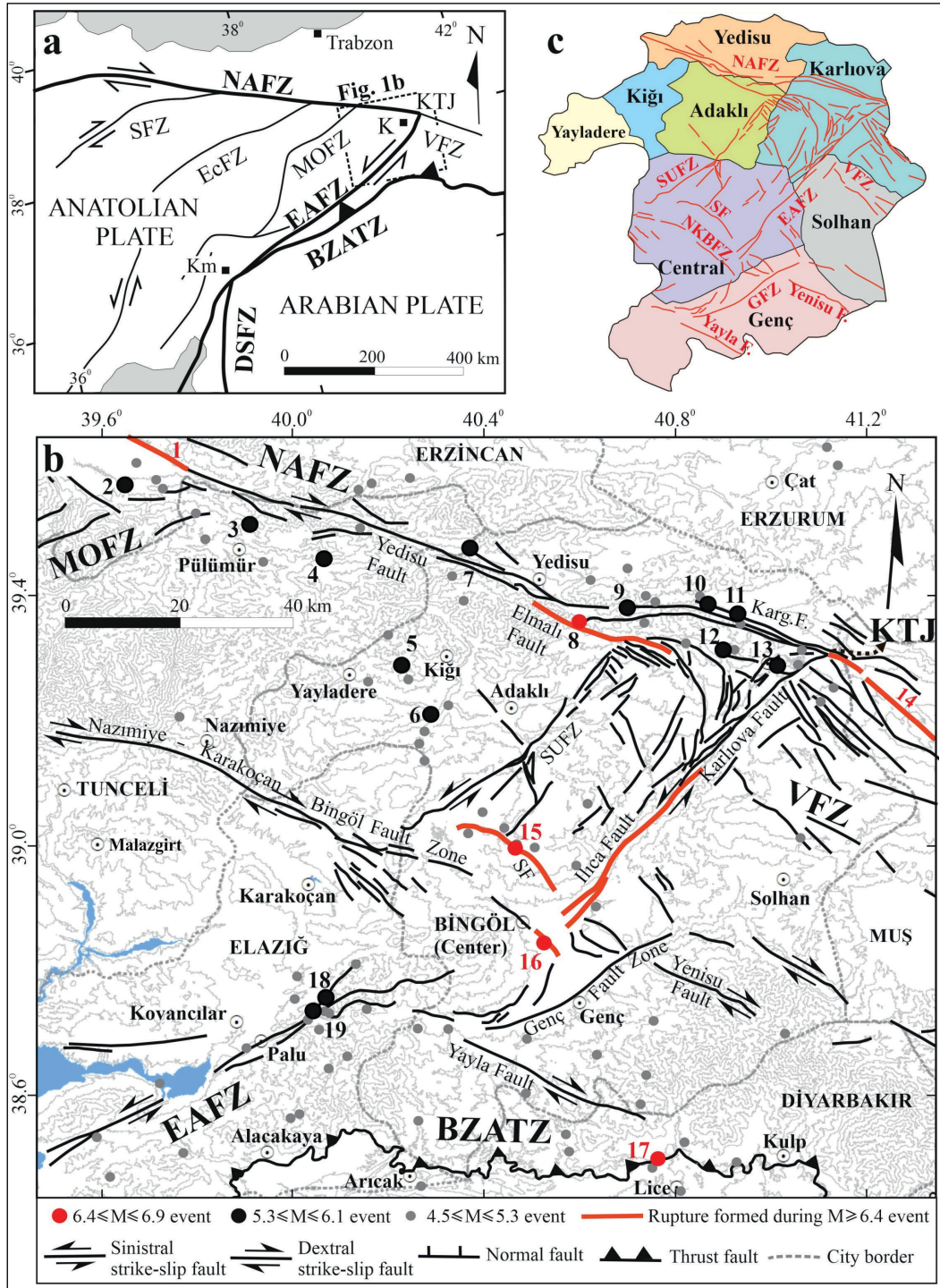


Figure 1- a) Simplified active tectonic map of Eastern and Southeastern Türkiye. Thick lines indicate plate boundary fault zones. Thin black lines are faults formed in the Anatolian Plate. b) The active fault map of the Bingöl and its surrounding. Gray lines are the elevation contours. For the location, see Figure 1a. The faults and their names are adapted from Emre et al. (2013) except Genç Fault Zone which is from Akbayram et al. (2022a). The earthquake data of numbered events are given in Table 1. Please note that the epicentre of events 1 and 15 are outside the map (cf., Table 1). The epicentre locations of events are borrowed from the online catalogue of the Kandilli Observatory and Earthquake Research Institute of Boğaziçi University (KOERI, 2022). c) The districts of Bingöl with the active fault zones. BZATZ: Bitlis Zagros Active Thrust Zone; DSFZ: Dead Sea Fault Zone; EAFZ: East Anatolian Fault Zone; EcFZ: Eciş Fault Zone; GFZ: Genç Fault Zone; K: Karlıova; Karg. F.: Kargapazarı Fault; Km: Kahramanmaraş; KTJ: Karlıova Triple Junction; MOFZ: Malatya Ovacık Fault Zone; NAFZ: North Anatolian Fault Zone; NKBZFZ: Nazımiye Karakoçan Bingöl Fault Zone; SF: Sudüğünü Fault; SFZ: Sungurlu Fault Zone; SUFZ: Sancak Uzunpinar Fault Zone; VFZ: Varto Fault Zone.

Table 1- The seismic data of $M \geq 5.3$ earthquakes occurred along the area shown in Figure 1b, recorded in the instrumental period. 1: The epicentres of these events are outside Figure 1b, however, part of their rupture is shown in Figure 1b.

Event no	Magnitude	Date (dd/mm/yy)	Epicenter (N°) - (E°)	References
1 ¹	7.9	26/12/1939	39.80 - 39.51	Kalafat et al. (2009), KOERI (2022)
2	6.1	27/01/2003	39.58 - 39.66	Kalafat et al. (2009), KOERI (2022)
3	5.8	15/03/1992	39.53 - 39.93	Tan et al. (2008), KOERI (2022)
4	5.7	05/12/1995	39.43 - 40.11	Tan et al. (2008), KOERI (2022)
5	5.3	02/12/2015	39.29 - 40.23	Altuncu et al. (2019)
6	5.3	06/25/2021	39.17 - 40.22	KOERI (2022)
7	5.9	26/07/1967	39.50 - 40.40	Eyidogan et al. (1991), McKenzie (1972), AFAD (2021)
8	6.9	17/08/1949	39.39 - 40.61	Ambraseys and Jackson (1998), Nalbant et al. (2002)
9	5.9	14/06/2020	39.37 - 40.74	Akbayram et al. (2022b)
10	5.4	23/03/2005	39.41 - 40.80	Demirtaş (2019), KOERI (2022)
11	5.6	12/03/2005	39.41 - 40.86	Demirtaş (2019), KOERI (2022)
12	5.9	14/03/2005	39.41 - 40.81	Demirtaş (2019), KOERI (2022)
13	5.7	06/06/2005	39.38 - 40.84	KOERI (2022)
14	6.9	19/08/1966	39.17 - 41.56	Tan et al. (2008), KOERI (2022)
15	6.4	01/05/2003	39.04 - 40.53	Kalafat et al. (2009), KOERI (2022)
16	6.8	22/05/1971	38.83 - 40.52	Taymaz et al. (1991), KOERI (2022)
17	6.0	06/09/1975	38.51 - 40.77	Tan et al. (2008), KOERI (2022)
18	6.1	08/03/2010	38.76 - 40.08	Tan et al. (2011), KOERI (2022)
19	6.8	08/03/2010	38.70 - 40.05	USGS (2022)

that applies a simple point process approach to various properties of documented seismicity (Hagiwara, 1974; Rikitake, 1974; Utsu, 1984; Anagnos and Kiremidjian, 1988; Campbell et al., 2002; Çobanoğlu et al., 2006;). The best-fit statistical models can be used to predict long-term earthquake generation process in a given area (Hainzl et al., 2006; Shelly et al., 2007; Wu et al., 2013). Gumbel (Gumbel, 1941), Gaussian (Rikitake, 1974), Lognormal (Nishenko and Buland, 1987), Gamma (Bak et al., 2002; Utsu, 1984), and Weibull (Hagiwara, 1974; Rikitake, 1974) statistical distributions of earthquakes used for computation of conditional probabilistic time-dependent seismic renewal models for future earthquakes (Parvez and Ram, 1999; Çobanoğlu et al., 2006; Tripathi, 2006; Yadav et al., 2010; Pasari and Dikshit, 2015, 2018). Determination of a suitable distribution model, which gives the best model for a given area, is important (Pasari and Dikshit, 2018) not only for forecasting future earthquakes but also for probabilistic seismic hazard analyses. The history and global applications of probabilistic modelling was summarized recently in Çoban and Sayıl (2020a, 2020b). Probabilistic seismic hazard analysis studies mainly focus on large sections (usually for hundreds of kilometers) of major faults (or deformation areas) such as North Anatolian Fault Zone (NAFZ), East Anatolian Fault Zone (EAFZ), Aegean Extensional Province and East Anatolian

High Plateau (e.g., Öztürk et al., 2008; Polat et al., 2008; Öztürk and Bayrak, 2012; Şahin and Öksüm, 2021; Alkan and Bayrak, 2022; Çoban and Sayıl, 2020a, 2020b; Öztürk, 2011).

In this study, our aim is to make the best-fit statistical models to predict long-term earthquake potential in and around the Bingöl city (Figure 1b). Even though the seismicity in Bingöl is well-documented until now, there is no study concentrated solely on the probabilistic earthquake forecasting in this area. One study that conducted probabilistic seismic hazard analysis within the City of Bingöl (Balun et al., 2020) obtained parameters using various attenuation relationships and discussed the earthquake codes. In this study, we use the earthquake data of the Kandilli Observatory and Earthquake Research Institute of Boğaziçi University (KOERI, 2022) and compared the Gumbel, Gaussian (Normal), Lognormal, Gamma, and Weibull distributions to define the best probability distribution for each district of Bingöl. As a result, we identified the best-fitting probability model for the studied catalogue and discussed earthquake forecasting in the study area. Finally, we have calculated return periods and discussed their correlation with the available paleo-seismological data.

2. Short Note on the Seismicity of Bingöl in the Instrumental Period

Figure 1b shows the active fault map of the city of the Bingöl city and surrounding. The red faults are the ruptured fault segments during $6.4 \leq M \leq 6.9$ events according to the MTA active fault database (Emre et al., 2013). All of the other faults (black lines in Figure 1b) are active faults that did not rupture in the instrumental period. Hence, they can be the sources of the next major earthquakes (Akbaşram et al., 2022a). Bingöl city has eight districts; namely Adaklı, Central, Genç, Karlıova, Kiğı, Solhan, Yayladere and Yedisu (Figure 1c). In this study, we have calculated the earthquake statistics for each district. Thus, in this section, we introduce the faults and their seismicity based on the districts they are located.

2.1. The Seismicity of the NAFZ in Karlıova, Yedisu and Adaklı Districts of Bingöl

According to Emre et al. (2013), the destructive 6.9 Ms, 1949 earthquake occurred on the Elmalı Fault of the NAFZ lying along the Adaklı and Karlıova District of Bingöl (Figure 1b-1c and Table 1). Others suggested that this earthquake occurred on the Kargapazarı or Yedisu Faults of Karlıova and Yedisu Districts (Ambraseys, 1989; Ambraseys and Jackson, 1998; Barka et al., 1987; Nalbant et al., 2002). The epicentre of 5.9 Ms, 1967 Pülümür earthquake (Ambraseys, 1975) that occurred outside of Bingöl is also very close to Yedisu District. The most recent moderate earthquake (5.9 Mw) occurred on the faults of the NAFZ cropping out along the Karlıova District on 14 June 2020 (AFAD, 2021; KOERI, 2022). These moderate earthquakes are not capable of releasing the strain accumulated in the NAFZ in Bingöl (Akbaşram et al., 2022b). Previously, the faults of the NAFZ in Bingöl are reported as seismic gaps (Sançar et al., 2009; Zabcı et al., 2017). Zabcı et al. (2017) mapped a 75-km-long throughgoing fault in the seismic gap of the NAFZ and suggested that it is capable of creating a 7.2 Mw earthquake.

2.2. The Seismicity of the EAFZ in Central, Karlıova and Genç Districts of Bingöl

The devastating May 22, 1971, Bingöl (Mw 6.8) earthquake occurred on the İlica Fault of the EAFZ in the Central District of Bingöl (Figure 1b-1c and Table 1) (Arpat and Şaroğlu, 1972; Taymaz et al.,

1991). The maximum intensity of the earthquake reached VIII (Mercalli scale) in the Central District where 878 people died and 9111 buildings became unusable (AFAD, 2021; KOERI, 2022). Towards NE, along the Karlıova Fault (Figure 1b) of the EAFZ, the last major earthquake (7.2 Ms) was documented in 1866 (Ambraseys and Jackson, 1998). The faults of the EAFZ between the southwestern end of the İlica Fault and Palu have not been ruptured in the last 160 years (Akbaşram et al. 2021). These faults are interpreted as a part of the Bingöl Seismic Gap (BSG) (Nalbant et al., 2002; Akbaşram et al., 2021; Duman and Emre, 2013). Although it is not included in the active fault database of Türkiye, both the morphotectonic analyses (Kıranşan et al., 2021) and seismic data suggest that the Genç Fault Zone (GFZ) (Figure 1b-1c) is also active (Herece 2008; Akbaşram et al., 2022a). Recently, GFZ is interpreted as an important component of the BSG (Akbaşram et al., 2022a). Two moderate earthquakes (6.1 and 5.6 Ms) occurred in 2010 along the BSG, very near to Central District of Bingöl City (Events 18, and 19 in Figure 1b and Table 1) (Tan et al., 2011). The events caused the death of 42 people and severely damaged more than 4000 buildings around the epicenter (AFAD, 2021; KOERI, 2022). Nevertheless, these events are hardly capable of releasing the strain accumulated (Nalbant et al., 2002) in the BSG following 1971 earthquake (Akbaşram et al., 2021).

2.3. The Seismicity of the Faults Located in the Anatolian Plate in Adaklı, Central, and Karlıova Districts of Bingöl

Bingöl also comprises some intra-plate, NW-SE trending dextral and NE-SW trending sinistral active faults that formed at the easternmost part of the Anatolian Plate (Figure 1) (Dewey and Şengör, 1979; Şengör, 1979; Şengör et al., 1985; Emre et al., 2013; Sançar et al., 2020). The Nazımiye Karakoçan Bingöl Fault Zone (NKBFZ) belongs to the NW-SE trending dextral fault family, and its southernmost part reaches the Central District of Bingöl (Figure 1b-1c) (Emre et al., 2013). The instrumental seismicity of the NKBFZ has been documented very recently. On January 31, 2022, a moderate (4.7 Mw) earthquake has occurred near Karakoçan on the NKBFZ (KOERI, 2022). Along the Sudüğünü Fault (SF), another NW-SE trending dextral fault mapped in the Central District (Figure 1b-1c), a disastrous earthquake (6.4 Ms) occurred on May 1, 2003 (Table 1) (Akkar et al., 2008; Kalafat et al.,

2009; Ulusay and Aydan, 2005; Utkucu et al., 2018). The maximum intensity of the earthquake reached VIII (Mercalli scale) in the Central District where 176 people died, and 6000 buildings became unusable (AFAD, 2021; KOERI, 2022). The Sancak Uzunpınar Fault Zone (SUFZ), a NE-SW trending 50-km-long sinistral fault zone (Emre et al., 2013; Selçuk et al., 2021), lies along the Central and Adaklı Districts (Figure 1b-1c). The Holocene activity of the SUFZ was recently documented by a paleo-seismological trench study (Selçuk et al., 2021). In addition to the aforementioned above, there are some other oblique active faults mapped in the Karlıova district near KTJ (Figure 1b-1c) (Emre et al., 2013). Even though there is no discussion on their active nature (Emre et al., 2013), their instrumental seismicity needs further geophysical analyses such as relocation because they are located in a region of complex faulting, very close to KTJ.

2.4. The Seismicity of VFZ, Yayla, Yenisu Faults in Genç, Karlıova and Solhan Districts

The NW-SE trending dextral faults are not limited to the Anatolian Plate in Bingöl (Figure 1b-1c). Many parallel faults of the Varto Fault Zone (VFZ) are in contact with the NAFZ and the EAFZ at the KTJ, both in Karlıova and Solhan Districts (Figure 1b-1c). The fault structure and seismicity of the VFZ discussed in detail in several studies (Emre et al., 2013; Gürboğa, 2016; Sançar et al., 2015; Seyitoğlu et al., 2019). The epicentre of the devastating Varto earthquake (6.9 Ms) in 1966, located outside Bingöl (Figure 1b), overlaps one of the faults of the VFZ (Table 1). However, its rupture reached Karlıova District of Bingöl (Figure 1b). The tectonic activity of the Yayla and Yenisu Faults located in the Genç District (Figure 1b-1c) is poorly known and needs further study (Emre et al., 2013).

3. Data and Method

In this study, we use the open earthquake database of KOERI. We divided the dataset into there as $1 \leq M < 3$ earthquakes, $3 \leq M$ earthquakes, and $1 \leq M$ earthquakes. In this study, earthquake magnitude classification is based on whether earthquakes can be felt without any instrumentation. According to the Mercalli classification, $3 \leq M$ earthquakes are usually felt without any instrument, while others can only be detected with instruments. As mentioned earlier, we

have determined the earthquake statistics for each district of Bingöl (Table 2). It is important to note that, in the KOERI database, the $3 \leq M$ earthquakes have been recorded since 1935, whereas the $1 \leq M < 3$ earthquakes have been recorded since 2001. The earthquake time periods recorded for each data set based on magnitude are given in Table 2 for each district. The maximum earthquake number (1393) and the highest earthquake magnitude (6.8) are observed in the Central District (Table 2). Karlıova District where KTJ is located, has maximum number of $1 \leq M < 3$ earthquakes. Although maximum earthquake magnitude for Genç District is only 4.9 M, the mean magnitude of $3 \leq M$ earthquakes are the maximum (3.7 M). Additionally, Genç District has maximum standard deviation for $1 \leq M$ earthquakes. A significant earthquake activity is observed, although there is no reported active fault in Kiğı District in the widely used active tectonic map of Türkiye released by Emre et al. (2013) (Table 2). The maximum earthquake magnitude reaches 5.7 M, and a significant number (654) of events have been documented in Kiğı District since 2000 (Table 2). Although the largest magnitude is 5.5 M, since 1935, the second lowest number of earthquakes has been documented in Solhan District compared to Genç, Yayladere and Yedisu Districts (Table 2). The lowest earthquake number (108) and maximum magnitude value (4.5) have been recorded in Yayladere District (Table 2). It is important to note that the recordings in Yayladere date back only to 1998.

Normal (Gauss), Lognormal, Gamma, Gumbel, and Weibull distributions are used here to analyze earthquake risk for all districts of Bingöl province. Since the study area is quite small, there is not sufficient recorded earthquake data to use conditional probability. In this study, maximum earthquake magnitudes are used instead of earthquake recurrence times for the earthquakes above certain magnitudes measured through years.

3.1. Normal (Gauss) Distribution

Natural events usually fit with the Gauss distribution. The normal distribution is a continuous function dependent X random variable. $f(X)$ gives probability values of a random variable using mean (μ) and standard deviation (σ) (Eq.1). The method has been widely used since the eighteenth century and developed by German mathematician Gauss and his colleagues (Kottegoda and Rosso, 2008).

Table 2- Earthquake statistics for each district of Bingöl.

Location	Earthquakes	Measured Years	Earthquake number	Mean (±0.1)	Maximum Magnitude	Standard Deviation (±0.01)
Adakh	$1 \leq M < 3$	2001-2021	182	2.2	2.9	0.48
	$3 \leq M$	1935-2020	58	3.5	5.7	0.66
	$1 \leq M$	1935-2021	240	2.5	5.7	0.78
Genç	$1 \leq M < 3$	2000-2021	146	2.2	2.9	0.45
	$3 \leq M$	1964-2020	52	3.7	4.9	0.69
	$1 \leq M$	1964-2021	198	2.6	4.9	0.82
Karlhova	$1 \leq M < 3$	2000-2021	868	2.2	2.9	0.52
	$3 \leq M$	1949-2020	323	3.4	6.0	0.58
	$1 \leq M$	1949-2021	1189	2.6	6.0	0.76
Kiğı	$1 \leq M < 3$	2000-2021	654	2.1	2.9	0.37
	$3 \leq M$	1907-2020	90	3.5	5.7	0.61
	$1 \leq M$	1907-2021	744	2.3	5.7	0.62
Central	$1 \leq M < 3$	2000-2021	708	2.4	2.9	0.48
	$3 \leq M$	1971-2021	685	3.3	6.8	0.37
	$1 \leq M$	1971-2021	1393	2.8	6.8	0.64
Solhan	$1 \leq M < 3$	2002-2021	126	2.3	2.9	0.48
	$3 \leq M$	1954-2014	30	3.6	5.5	0.62
	$1 \leq M$	1954-2021	156	2.5	5.5	0.72
Yayladere	$1 \leq M < 3$	2002-2021	84	2.2	2.9	0.38
	$3 \leq M$	1998-2019	24	3.4	4.5	0.39
	$1 \leq M$	1998-2021	108	2.5	4.5	0.62
Yedisu	$1 \leq M < 3$	2002-2021	643	2.0	2.9	0.49
	$3 \leq M$	1935-2021	95	3.5	5.3	0.56
	$1 \leq M$	1935-2021	728	2.2	5.3	0.70

$$f(X) = \frac{1}{\sigma\sqrt{2\pi}} \exp\left[-\frac{1}{2}\left(\frac{x-\mu}{\sigma}\right)^2\right] f(X) = \frac{1}{\sqrt{f2\pi}} \exp\left[-\frac{1}{2}\left(\frac{x-\mu}{\sigma}\right)^2\right] \rho_p = \frac{F_G}{F_p} \quad -\infty < x < \infty$$

(1)

3.2. Lognormal Distribution

Some non-normal variables can be fitted to the Normal distribution using logarithmic transformations (Eq.2). The probability distribution function of Lognormal is given with Eq.3. μ_y and σ_y represent mean and standard deviation of Y random variables.

$$Y = \ln(x) \rho_p = \frac{F_G}{F_p} \quad (2)$$

$$f(x) = \frac{1}{x\sigma_y\sqrt{2\pi}} \exp\left[-\frac{(\ln x - \mu_y)^2}{2\sigma_y^2}\right] \quad x \gg 0$$

$$(3) \rho_p = \frac{F_G}{F_p}$$

3.3. Gamma Distribution

Gamma distribution is frequently used to examine skewed distributions. Shape and scale parameter is shown as α and β for random variables distributions (Eq.4). Gamma function, $\Gamma(\alpha)$, is calculated with Eq.5. The mean and standard deviation value of the Gamma distribution is obtained using Eqs.6 and 7.

$$f(x) = \frac{1}{\beta^\alpha \Gamma(\alpha)} x^{\alpha-1} e^{-x/\beta} \quad x \geq 0 \quad (4)$$

$$\Gamma(\alpha) = \int_0^\infty x^{\alpha-1} e^{-x} dx \quad (5)$$

$$Mean(x) = \alpha\beta \tag{6}$$

$$Var(x) = \alpha\beta^2$$

$$(7)Var(x) = \alpha\beta^2E(x) = \alpha\beta$$

3.4. Gumbel Distribution

Gumbel distribution is a special case of a Generalized Extreme Value distribution. It is used for extreme value problems. The cumulative probability function is seen on Eq.8 (Gumbel, 1941). In here, x represents random variable, and α shape parameter, and β location parameter. ($\alpha = \frac{\sigma}{1.283}$ and $\beta = \mu - \frac{0.577}{\alpha}$)

$$F(x) = \exp \left\{ -\exp \left[-\left(\frac{x}{\alpha} - \xi \right) \right] \right\}$$

$$\kappa = 0 \quad F(x) = \exp \left(-\exp \exp \left(-\frac{x-\beta}{\alpha} \right) \right) \tag{8}$$

3.5. Weibull Distribution

Weibull distribution is used frequently to determine material service life and wind potentials in the literature. Probability distribution function is given by Eqs. 9. If $x \geq 0$, α represents scale parameter and, β , shape parameter. Scale and shape parameters can be obtained from Eqs. 10 and 11. $\Gamma(\alpha)$ represents Gamma Function (Eq. 5).

$$f(x) = \alpha\beta x^{\beta-1} e^{-\alpha x^\beta} \tag{9}$$

$$E(x) = \beta\Gamma\left(1 + \frac{1}{\alpha}\right) \tag{10}$$

$$Var(x) = \beta^2 \left\{ \Gamma\left(1 + \frac{2}{\alpha}\right) - \left[\Gamma\left(1 + \frac{1}{\alpha}\right) \right]^2 \right\} \tag{11}$$

Model parameters of Normal (Gaussian), Lognormal, Gamma, Gumbel and Weibull distributions are calculated according to the method of moments. The fitting of the mentioned probability distributions is tested by mean absolute errors (MAE), mean percentage errors (MPE) and Kolmogorov-Smirnov minimum distances (KS). In Eqs. 12, 13, and 14, $\hat{F}(x)$ gives cumulative empirical probability function, $F(x)$, cumulative theoretical distribution function and n , data number, and D , Kolmogorov-Smirnov test statistics. If KS test statistics, D , is smaller than its tabulated values, the empirical probability values agree with the cumulative probability values. MPE

values smaller than 5% can be accepted confidently for statistical studies.

$$MAE = \frac{1}{n} \sum_{i=1}^n |\hat{F}(xi) - F(xi)| \tag{12}$$

$$MPE = \frac{1}{n} \sum_{i=1}^n \left(\frac{\hat{F}(xi) - F(xi)}{\hat{F}(xi)} \right) \times 100 \tag{13}$$

$$D = (|\hat{F}(xi) - F(xi)|) \quad 1 \leq i \leq n \tag{14}$$

4. Results and Discussion

4.1. Cumulative Probability Distributions

Figure 2 shows the empirical and theoretical cumulative probability distribution values of the Central District of Bingöl calculated for all of the distribution functions mentioned in previous sections. For sake of brevity, mean absolute errors for other districts are only given in Table 3, and the cumulative probability distribution values for these districts are not shown in separate figures. In Table 3, the lowest mean absolute errors, KS test statistics, and MPE values lower than 5% for each district are shown in bold indicating the best-fit model for all districts. In Figure 2, blue scatter points give empirical cumulative probability values according to the earthquake magnitudes, and black lines represent continuous theoretical cumulative probability values. A data length as “ n ” and an ordered data order as “ i ”, empirical cumulative probability values are obtained as $(\frac{i}{n+1})$. Theoretical cumulative probability values are calculated using Normal, Lognormal, Gamma, Weibull, and Gumbel probability distribution functions. Comparing the calculated probability distribution functions, a probability distribution function with the least mean absolute error and KS test statistics, D , is selected as the most suitable probability distribution provided that its MPE values are smaller than absolute %5. The Gumbel probability distribution best fits measured earthquake magnitudes of the Central District of Bingöl, and as a result, the black line best fits to blue scatter points in the Gumbel distribution (Figure 2). The mean absolute error and KS test statistics of the measured earthquake magnitudes of the Central District of Bingöl is minimum (0.036 and 0.118<0.274) for Gumbel and maximum (0.072 and 0.189) for Weibull distributions (Table 3). The Gumbel distribution also gives best fits for earthquake magnitudes of Karlıova (0.031 and 0.075<0.270) and Adaklı (0.032 and 0.078<0.286) Districts. The Weibull distribution has maximum

mean absolute errors and KS statistics for Karlıova (0.071 and 0.143) and Adaklı (0.083 and 0.172) Districts measured earthquake magnitudes similar to the Central District. However, the earthquake magnitudes of the Genç (0.034 and 0.103<0.274) and Yayladere (0.028 and 0.072<0.278) districts best fit the Weibull distributions. The lognormal distribution has the minimum mean absolute errors of earthquake magnitudes for Kiğı (0.026) and Solhan (0.036)

districts, which have the smallest KS statistics (0.075 and 0.092) for Gumbel distribution. Since the MPE values for Lognormal distribution are lower than Gumbel distribution, the most appropriate distribution for these districts is selected as Lognormal distribution. The earthquake magnitudes of the Yedisu District best fit Normal distribution with mean absolute errors (0.045) and KS statistics (0.093<0.270).

Table 3- Mean absolute, percentage errors, and Kolmogorov-Smirnov test statistics of probability distributions of earthquake magnitudes of all the districts of Bingöl.

Districts	Measured Years	Mean Absolute Errors				
		Normal	Lognormal	Gamma	Weibull	Gumbel
Central	1996-2020	0.062	0.041	0.052	0.072	0.036
Adaklı	1999-2020	0.063	0.049	0.054	0.083	0.032
Genç	1999-2020	0.042	0.053	0.049	0.034	0.075
Karlıova	1995-2020	0.059	0.041	0.045	0.071	0.031
Kiğı	1998-2020	0.034	0.026	0.027	0.047	0.033
Solhan	2001-2020	0.042	0.036	0.037	0.057	0.042
Yayladere	1998-2020	0.028	0.034	0.033	0.028	0.051
Yedisu	2000-2020	0.045	0.048	0.047	0.053	0.067
Kolmogorov-Smirnov minimum distances						
Districts	Measured Years	Normal	Lognormal	Gamma	Weibull	Gumbel
Central	1996-2020	0.166	0.142	0.141	0.189	0.118
Adaklı	1999-2020	0.139	0.111	0.124	0.172	0.078
Genç	1999-2020	0.131	0.159	0.143	0.103	0.166
Karlıova	1995-2020	0.125	0.101	0.102	0.143	0.075
Kiğı	1998-2020	0.111	0.089	0.101	0.122	0.075
Solhan	2001-2020	0.155	0.122	0.133	0.184	0.092
Yayladere	1998-2020	0.074	0.112	0.103	0.072	0.143
Yedisu	2000-2020	0.093	0.113	0.104	0.122	0.151
Mean Percentage Errors						
Districts	Measured Years	Normal	Lognormal	Gamma	Weibull	Gumbel
Central	1996-2020	-4.90%	0.31%	-6.43%	-3.39%	-4.17%
Adaklı	1999-2020	-1.53%	1.03%	-2.46%	1.13%	0.16%
Genç	1999-2020	-0.07%	-2.73%	-0.99%	2.58%	-4.44%
Karlıova	1995-2020	-1.90%	1.70%	-2.52%	-1.44%	1.75%
Kiğı	1998-2020	1.18%	3.43%	0.72%	2.16%	3.71%
Solhan	2001-2020	3.35%	4.00%	2.87%	4.10%	5.06%
Yayladere	1998-2020	4.36%	3.47%	4.81%	4.26%	6.92%
Yedisu	2000-2020	3.67%	3.87%	3.95%	4.38%	7.81%

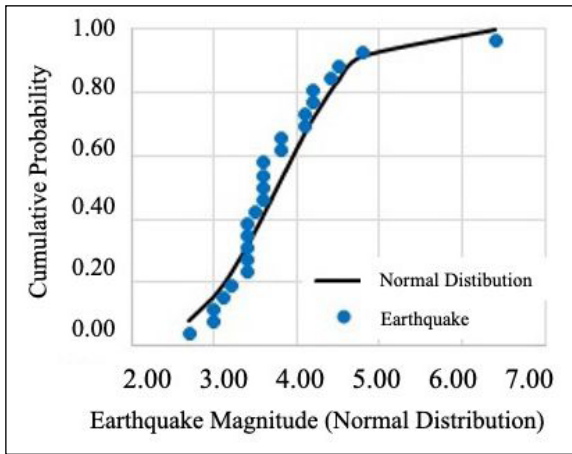


Figure 2- Cumulative probability distribution functions for maximum earthquake magnitudes of the Central District of Bingöl.

In order to determine the earthquake activity for each district of Bingöl, the recorded $1 \leq M < 3$ earthquakes are analysed without their probability distributions. Figure 3 shows the number of $1 \leq M < 3$ earthquakes recorded in each district of Bingöl since 2001 in order to compare the seismic activity of districts in the study area during the same recording period. In this figure, the horizontal axis shows the years and the vertical axis shows the earthquake numbers. $1 \leq M < 3$ earthquake numbers are high for the Central District in 2003 and in 2018 compared to other years. Most of the $1 \leq M < 3$ earthquakes recorded in 2003 are the aftershocks of May 1, 2003 (6.4 Ms) earthquake (Table 1) along Sudüğünü Fault (SF) in the Central District (Ulusay and Aydan, 2005; Akkar et al., 2008; Kalafat et al., 2009; Utkucu et al., 2018).

$1 \leq M < 3$ earthquake numbers of Adaklı and Solhan Districts change regularly, no significant increase is observed on the graph. In the Genç and Yayladere Districts, $1 \leq M < 3$ earthquake numbers are usually low with a significant increase in 2015. Also, the maximum $1 \leq M < 3$ earthquake numbers occurred in the Kiğı district in 2015, and the maximum $1 \leq M$ earthquake magnitude is 5.5 for the same year. In 2005 and 2020, the maximum $1 \leq M < 3$ earthquake number and the maximum $1 \leq M$ earthquake magnitude (5.9) was measured in the Karlıova District. The increase in earthquake numbers in these years can be explained by the occurrence of aftershocks of 12-14 March 2005 (5.7 Ml and 5.9 Ml respectively) (Demirtaş, 2019; KOERI, 2022), and 14 June 2020, 5.9 Mw (Akbaş et al., 2022b; AFAD 2021; KOERI 2022) events.

In the Yedisu District, $1 \leq M < 3$ earthquake number is maximum as in Karlıova District. The maximum earthquake magnitude of $1 \leq M$ (4.4) occurs in 2020 with the maximum number of earthquakes of $1 \leq M < 3$ because some of the aftershocks of 5.9 Mw, 2020 earthquake are superimposed in the Yedisu District (Akbaş et al., 2022b).

4.2. The Return Periods Correlated with Maximum Earthquake Magnitudes and Their Discussion on Available Paleo-Seismological Data

In this section, we have given the return periods, and maximum annual earthquake magnitudes according to return periods for each district of Bingöl (Figure 4). However, these values are only meaningful when correlated with available paleo-seismological data that we also discuss in this section. In Figure 4, the horizontal axis represents return periods and the vertical axis maximum earthquake magnitudes according to a selected return period. We have selected the return periods as 10, 50, 100, 250, and 1000 years. For example, according to the figure, the expected maximum earthquake magnitude for the Central District of Bingöl is 7.5 for 1000 years return period.

The earthquake magnitude maxima obtained from the Central District, as 4.7, 5.7, 6.1, 6.7, and 7.5 for 10, 50, 100, 250, and 1000 years return periods. There are four active fault zones mapped in the Central District; the EAFZ, the NKBZF, the SF, and the SUFZ (Figure 1b-1c). Unfortunately, there are no published paleo-seismology results along the segments of the EAFZ, the NKBZF, and the SF in the Central District. However, paleo-seismology studies held along the Palu-Hazar Lake Segment of the EAFZ suggest that every 100 to 365 years a large ($M > 7$) earthquake occurs on this fault zone (Çetin et al. 2003). A study dating seismo-turbidites of Hazar Lake suggests ~190 years of earthquake recurrence in the last 3800 years (Hubert-Ferrari et al. 2020). If we combine these findings and accept that every ~230-250 years (the average of these values) a large earthquake occurs in the faults of the EAFZ in Bingöl (Taymaz et al. 1991).

In Karlıova district, the maximum earthquake magnitude maxima obtained as 5.1, 6.2, 6.6, 7.2, and 8.2 for 10, 50, 100, 250, and 1000 years return

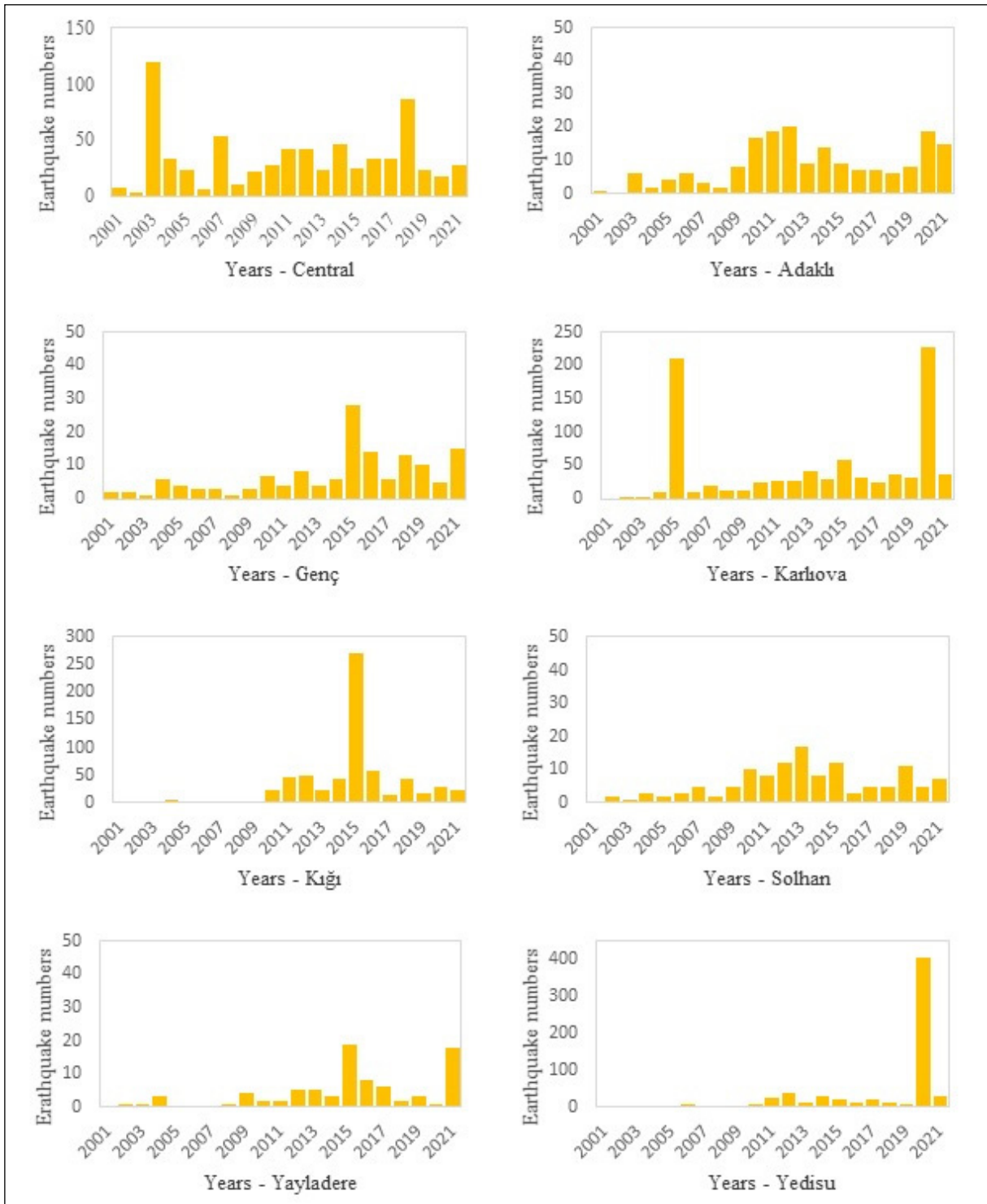


Figure 3- Numbers of $1 \leq M < 3$ earthquakes occurred between 2001 and 2020 in the Districts of Bingöl.

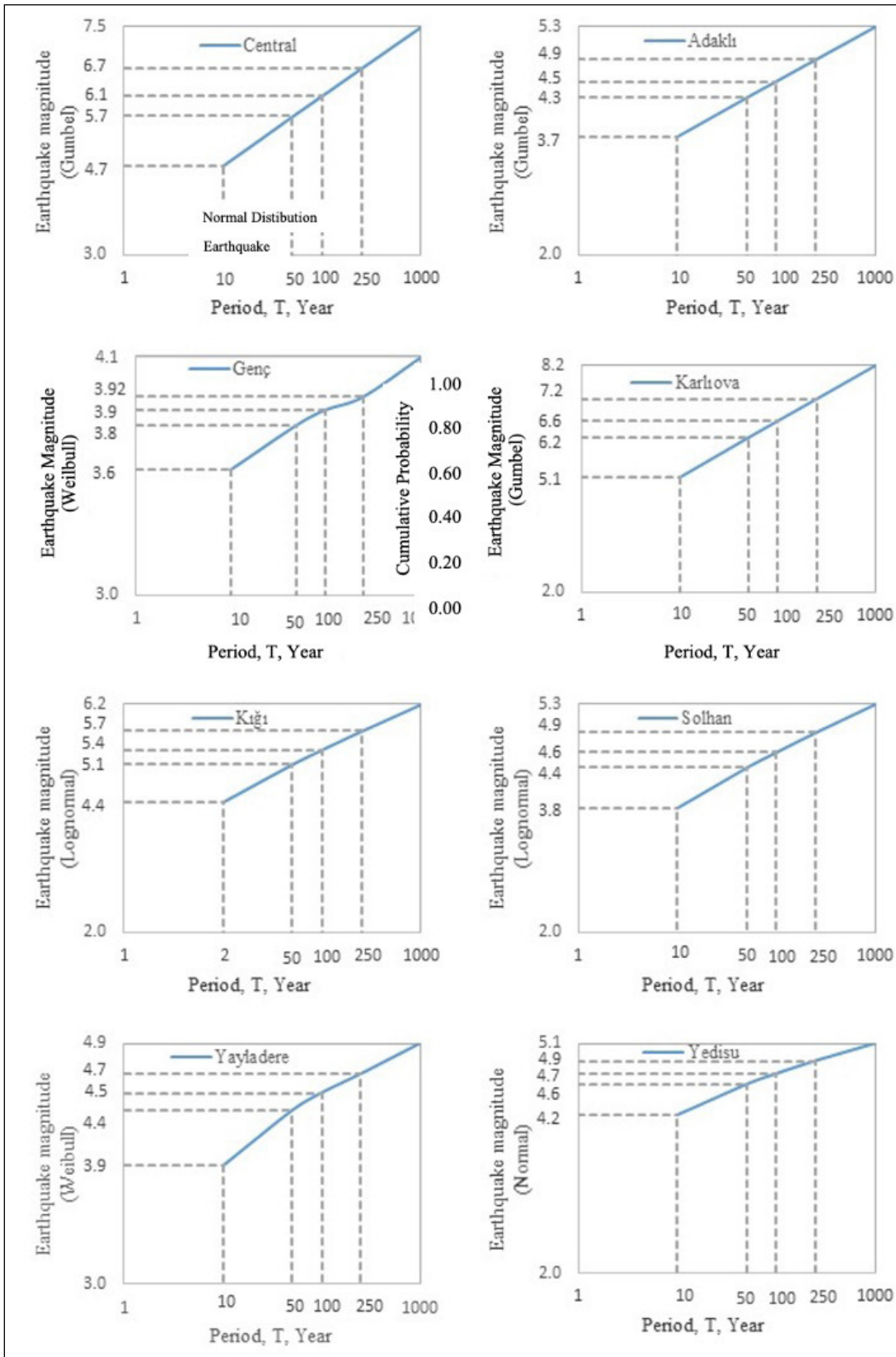


Figure 4- The maximum annual earthquake magnitudes according to return periods for each district of Bingöl. The paleoseismological trench study held along the SUFZ suggests at least two main events in the Holocene without giving a recurrence interval (Selçuk et al., 2021).

periods. The Karlıova District hosts the KTJ where the pieces of both the NAFZ and the EAFZ mapped. The previous studies suggest an earthquake recurrence interval of 200 to 250 along most of the length of the NAFZ (cf., Zabcı et al., 2017). Hence, it is safe to choose the maximum earthquake value corresponding the 250 return period which is 7.2 M (Figure 4) as the probable magnitude of the next big earthquake occurred on the NAFZ and EAFZ in the Karlıova District. This magnitude is also in good correlation with the maximum expected earthquake value (7.2 M) calculated by Zabcı et al (2017).

The maximum earthquake magnitudes seem to be 5.1 M for the 1000-year return period in Yedisu District, where some important segments of the NAFZ were mapped (Figure 4). This is not compatible with the paleo-seismological trench results and empirical calculations of Zabcı et al (2017). The reason for this inconsistency is attributed to low quality seismic data in this region.

For Kiğı and Solhan Districts, maximum earthquake magnitudes fit the Lognormal distribution, and the earthquake magnitudes are 6.2 and 5.3 for the 1000-year return period. Weibull distributed Yayladere District's maximum earthquake magnitudes are 4.9 for the 1000-year return period. For the Genç District, the least maximum earthquake magnitude is calculated as 4.1 for the same return period. If 10-year return periods are examined, maximum earthquake magnitudes are calculated between 3.6 and 5.1 in all districts. This shows that perceptible earthquakes will occur once every ten years.

5. Conclusions

Determination of the 5 time-dependent probability distributions (Normal, Lognormal, Gamma, Gumbel, Weibull) and return periods of earthquakes for all districts of Bingöl give the following results. The best probability fit arises from the Gumbel distribution for Central, Karlıova, and Adaklı Districts. For the Genç District, where the least maximum earthquake magnitude is reported, the Weibull distribution gives the best fit. For the Central and Karlıova Districts, along which maximum earthquake magnitudes were reported and important faults of NAFZ and EAFZ were mapped, every 250 years a 6.6 M, and a 7.2 M occurs respectively. These results are in good correlation with

the results of paleo-seismological data reported along the NAFZ and the EAFZ. Earthquake magnitudes in the 250-year return period change among 3.9 (Genç), 4.9 (Adaklı), 4.9 (Solhan), 4.9 (Yedisu), 4.7 (Yayladere), 5.7 (Kiğı). Calculated maximum earthquake magnitudes show that buildings in Bingöl City and Karlıova district must be constructed more carefully than the other districts. For a 10-year return period, earthquake magnitudes reach to 3.6 and 5.1 in all districts suggesting that every decade a perceptible earthquake will occur in Bingöl. It is important to note that in the Yedisu District, the maximum earthquake magnitudes seem as 5.1 M for the 1000-year return period, incompatible with previously published findings. Significant changes in earthquake numbers in the Yedisu necessitate investigation of active faults, and seismicity in the zone.

Acknowledgement

We sincerely thank Kemal Kıranşan for supplying the elevation contours and city borders in Figure 1b, three anonymous reviewers, Editor-in-Chief Halim Mutlu, Associate Editors Şule Gürboğa, and Eren Pamuk for their valuable criticism and help during the review process.

References

- AFAD (Disaster and Emergency Management Presidency). <http://www.afad.gov.tr> (April 23,2021).
- Akbayram, K., Kıranşan, K., Özer, Ç., Varolgüneş, S. 2021. The surface deformation of the 2020 Doğanyol-Sivrice earthquake (Mw 6.8) and the earlier events suggest Mw<7.0 earthquakes do not create significant surface slip along the East Anatolian Fault Zone (unpublished).
- Akbayram, K., Bayrak, E., Pamuk, E., Özer, Ç., Kıranşan, K., Varolgüneş, S. 2022a. Dynamic sub-surface characteristic and the active faults of the Genç District locating over the Bingöl Seismic Gap of the East Anatolian Fault Zone, Eastern Turkey. *Natural Hazards* 114(1) ,825-847.
- Akbayram, K., Kıranşan, K., Varolgüneş, S., Büyükkapınar, P., Karasözen, E., Bayık, Ç. 2022b. Multi-disciplinary analyses of the rupture characteristic of 2020 June 14 Mw 5.9 Kaynarçınar (Karlıova, Bingöl) earthquake reveals NE-SW trending active faulting along the Yedisu Seismic Gap of the North Anatolian Fault Zone towards Turkish-

- Iranian Plateau. *International Journal of Earth Sciences* 1-21.
- Akkar, S., Boore, D. M., Gülkan, P. 2008. An evaluation of the strong ground motion recorded during the May 1, 2003 Bingol Turkey, earthquake. *Journal of Earthquake Engineering* 9, 173–197.
- Alkan, H., Bayrak, E. 2022. Coulomb stress changes and magnitude - frequency distribution for Lake Van region. *Bulletin of the Mineral Research and Exploration* 168, 141-156.
- Altuncu P. S., Aksarı, D., Ergün, T., Teoman, U. M., Pınar, A. 2019. The December 2nd, 2015 Bingöl, Eastern Anatolia-TURKEY, earthquake (Mw = 5.3): A rupture on optimally oriented fault plane. *Journal of Asian Earth Science* 173, 88–97.
- Ambraseys, N. 1970. Some characteristic features of the Anatolian fault zone. *Tectonophysics* 9, 143–165.
- Ambraseys, N. 1975. Studies in historical seismicity and tectonics. *Geodynamics*.
- Ambraseys, N. 1989. Temporary seismic quiescence: SE Turkey. *Geophysical Journal International* 96, 311–331.
- Ambraseys, N., Jackson, J. 1998. Faulting associated with historical and recent earthquakes in the Eastern Mediterranean region. *Geophysical Journal International* 133, 390–406.
- Anagnos, T., Kiremidjian, A. 1988. A review of earthquake occurrence models for seismic hazard analysis. *Probabilistic Engineering Mechanics* 3, 3–11.
- Arpat, E., Şaroğlu, F. 1972. The East Anatolian Fault System: thoughts on its development. *Bulletin of the Mineral Research And Exploration* 78, 33–39.
- Bak, P., Christensen, K., Danon, L., Scanlon, T. 2002. Unified scaling law for earthquakes. *Physical Review Letters* 88, 178501.
- Balun, B., Nemutlu, Ö.F., Sarı, A. 2020. Estimation of probabilistic hazard for Bingol province, Turkey. *Earthquakes and Structures* 18 (2), 223-231.
- Barka, A., Toksöz, M., Kadinsky-Cade, K., Gülen, L. 1987. The segmentation, seismicity and earthquake potential of the eastern part of the North Anatolian Fault Zone. *Bulletin of Earth Science* 14, 337–352.
- Campbell, K., Thenhaus, P., Bamhard, T., Hampson, D. 2002. Seismic hazard model for loss estimation and risk management in Taiwan. *Soil Dynamic Earthquake Engineering* 22, 743–754.
- Çetin, H., Güneyli, H., Mayer, L. 2003. Paleoseismology of the Palu-Lake Hazar segment of the East Anatolian fault zone, Turkey. *Tectonophysics* 374, 163-197.
- Çoban, K. H., Sayil, N. 2020a. Different probabilistic models for earthquake occurrences along the North and East Anatolian fault zones. *Arabian Journal of Geosciences* 13 (18), 1-16.
- Çoban, K. H., Sayil, N. 2020b. Conditional Probabilities of Hellenic Arc Earthquakes Based on Different Distribution Models. *Pure and Applied Geophysics* 177 (11), 5133–5145.
- Çobanoğlu, İ., Bozdağ, Ş., Dinçer, İ., Erol, H. 2006. Statistical Approaches to Estimate the Recurrence of Earthquakes in the Eastern Mediterranean Region. *İstanbul Yerbilimleri Dergisi* 19, 91–100.
- Demirtaş, R. 2019. 12 Mart 2005 (M=5.6), 14 Mart 2005 (M=5.9) ve 24 Mart 2005 (M=5.4) Karlıova (Bingöl) Depremleri. Ankara.
- Dewey, J., Şengör, A. 1979. Aegean and surrounding regions: complex multiplate and continuum tectonics in a convergent zone. *Geological Society of America Bulletin* 84–92.
- Duman, T. Y., Emre, Ö. 2013. The East Anatolian Fault: geometry, segmentation and jog characteristics. *Geological Society, London, Special Publications* 495–529.
- Emre, Ö., Duman, T., Özalp, S., Elmacı, H., Olgun, Ş., Şaroğlu, F. 2013. Active Fault Map of Turkey with an Explanatory Text 1:1.250.000 scale, Special Publication Series 30. General Directorate of Mineral Research and Exploration (MTA), Turkey.
- Eyidoğan, H., Guclu, U., Utku, Z., Degirmenci, E. 1991. Türkiye Büyük Depremleri Makro-Sismik Rehberi (1900–1988). ITU Maden Fakültesi Jeofizik Mühendisliği Bölümü, İstanbul.
- Gumbel, E. J. 1941. The Return Period of Flood Flows. *Annals of Mathematical Statistics* 12, 163-190.
- Gürboğa, Ş. 2016. The termination of the North Anatolian Fault System (NAFS) in Eastern Turkey. *International Geological Review* 58, 1557–1567.
- Hagiwara, Y. 1974. Probability of earthquake occurrence as obtained from a Weibull distribution analysis of crustal strain. *Tectonophysics* 23, 313–318.
- Hainzl, S., Scherbaum, F., Beauval, C. 2006. Estimating Background Activity Based on Interevent-Time Distribution. *Bulletin of the Seismological Society of America* 96, 313–320.

- Herece, E. 2008. Atlas of East anatolian fault. MTA Special Publication Series 13.
- Hubert-Ferrari A., Lamair, L., Hage, S., Schmidt, S., Çağatay, M. N., Avşar, U. 2020. A 3800 yr paleoseismic record (Lake Hazar sediments, eastern Turkey): Implications for the East Anatolian Fault Seismic Cycle. *Earth and Planetary Science Letters* 538, 116-152.
- Kalafat, D., Kekovalı, K., Güneş, Y., Yilmazer, M., Kara, M., Deniz, P., Berberoğlu, M. 2009. A catalogue of source parameters of moderate and strong earthquakes for Turkey and its surrounding area (1938–2008). Boğaziçi University, Kandilli Observatory and Earthquake Research Institute.
- Kırınşan, K., Akbayram, K., Avcı, V. 2021. Effects of Active Tectonism on Geomorphological Structure in Bingöl Basin and Its Surroundings. *Gümüşhane Üniversitesi Sosyal Bilimler Enstitüsü Elektronik Dergisi* 12, 1110–1129.
- KOERI (Kandilli Observatory and Earthquake Research Institute). <http://koeri.boun.edu.tr> (May 12, 2022).
- Kottegoda, N. T., Rosso, R. 2008. Applied Statistics for Civil and Environmental Engineers, Engineering.
- Köküm, M., Özçelik, F. 2020. An example study on re-evaluation of historical earthquakes: 1789 Palu (Elazığ) earthquake, Eastern Anatolia, Turkey. *Bulletin of the Mineral Research and Exploration*. 161, 157-172.
- McKenzie, D. 1972. Active tectonics of the Mediterranean region. *Geophysics Journal International* 30, 109–185.
- Nalbant, S., McCloskey, J., Steacy, S., Barka, A. 2002. Stress accumulation and increased seismic risk in eastern Turkey. *Earth Planetary Science Letters* 195, 291–298.
- Nishenko, S., Buland, R. 1987. A generic recurrence interval distribution for earthquake forecasting. *Bulletin of the Seismological Society of America* 77, 1382–1399.
- Öztürk, S., Bayrak, Y., Çınar, H., Koravos, G. C., Tsapanos, T. M. 2008. A quantitative appraisal of earthquake hazard parameters computed from Gumbel I method for different regions in and around Turkey. *Natural Hazards* 47 (3), 471–495
- Öztürk, S. 2011. Characteristics of seismic activity in the Western, Central and Eastern parts of the North Anatolian Fault Zone, Turkey: Temporal and spatial analysis. *Acta Geophysica* 59, 209–238.
- Öztürk, S., Bayrak, Y. 2012. Spatial variations of precursory seismic quiescence observed in recent years in the eastern part of Turkey. *Acta Geophysica* 60, 92–118.
- Parvez, I. A., Ram, A. 1999. Probabilistic Assessment of Earthquake Hazards in the Indian Subcontinent. *Pure and Applied Geophysics* 154, 23–40.
- Pasari, S., Dikshit, O. 2015. Earthquake interevent time distribution in Kachchh, Northwestern India. *Earth Planet and Space* 67, 1-17.
- Pasari, S., Dikshit, O. 2018. Stochastic earthquake interevent time modeling from exponentiated Weibull distributions. *Natural Hazards* 90, 823–842.
- Polat, O., Gök, E., Yılmaz, D. 2008. Earthquake hazard of Aegean Extension Region, Turkey. *Turkish Journal of Earth Science* 17, 593–614.
- Rikitake, T. 1974. Probability of earthquake occurrence as estimated from crustal strain. *Tectonophysics* 23, 299–312.
- Sançar, T., Zabcı, C., Akyüz, H., Karabacak, V., Altunel, E. 2009. Late Holocene Activity of Kargapazari Segment, Eastern Part of the North Anatolian Fault Zone, Bingöl, Turkey. *EGU General Assembly, Vienna*, 7710.
- Sançar, T., Zabcı, C., Akyüz, H., Sunal, G., Villa, I. 2015. Distributed transpressive continental deformation: The Varto Fault Zone, eastern Turkey. *Tectonophysics* 661, 99–111.
- Sançar, T., Zabcı, C., Akcar, N., Karabacak, V., Yeşilyurt, S., Yazıcı, M., Akyüz, H., Öztüfekçi Önal, A., Ivy-Ochs, S., Christl, M., Vockenhuber, C. 2020. Geodynamic importance of the strike-slip faults at the eastern part of the Anatolian Scholle: Inferences from the uplift and slip rate of the Malatya Fault. *Journal of Asian Earth Science* 188, 104091.
- Selçuk, A., Erturaç, M., Karabacak, V., Sançar, T., Kul, A., Yavuz, M. 2021. Active Tectonic Setting and Paleoseismicity of the Sancak-Uzunpazar Fault Zone. *Turkish Journal of Earthquake Research* 3, 75–91.
- Şahin, Ş., Öksüm, E. 2021. The relation of seismic velocity and attenuation pattern in the East Anatolian fault zone with earthquake occurrence: Example of January 24, 2020 Sivrice Earthquake. *Bulletin of the Mineral Research and Exploration* 165, 141-161.
- Şengör, A., 1979. The North Anatolian transform fault: its age, offset and tectonic significance. *Journal of Geological Society of London* 136, 269–282.

- Şengör, A. 1980. Türkiye neotektoniğinin esasları. Türkiye Jeoloji Kurumu Konferans Serisi 2. Ankara, 40.
- Şengör, A., Görür, N., Şaroğlu, F. 1985. Strike-slip faulting and related basin formation in zones of tectonic escape: Turkey as a case study, in: Biddle, K., Christie-Blick, N. (Eds.), *Strike-Slip Deformation, Basin Formation and Sedimentation*. Society of Economic Paleontologists and Mineralogists, Tulsa, OK, 227–264.
- Seyitoğlu, G., Esat, K., Kaypak, B., Moosarrez, T., Bahadır, A. 2019. Internal Deformation of Turkish-Iranian Plateau in the Hinterland of Bitlis-Zagros Suture Zone. *Developments in Structural Geology and Tectonics* 3, 161–244.
- Shelly, D., Beroza, G., Ide, S. 2007. Non-volcanic tremor and low-frequency earthquake swarms. *Nature* 446, 305–307.
- Tan, O., Tapırdamaz, M., Yörük, A. 2008. The Earthquake Catalogues for Turkey. *Turkish Journal Earth Science* 17, 405–418.
- Tan, O., Pabucu, Z., Tapırdamaz, M. C., Nan, S., Ergintav, S., Eyidoğan, H., Aksoy, E., Kuluöztürk, F. 2011. Aftershock study and seismotectonic implications of the 8 March 2010 Kovanclar (Elazğ, Turkey) earthquake (MW = 6.1). *Geophysical Research Letters* 38.
- Taymaz, T., Eyidoğan, H., Jackson, J. 1991. Source parameters of large earthquakes in the East Anatolian Fault Zone (Turkey). *Geophysical Journal International* 106, 537–550.
- Tripathi, J. 2006. Probabilistic assessment of earthquake recurrence in the January 26, 2001 earthquake region of Gujrat, India. *Journal of Seismology* 10, 119–130.
- Ulusay, R., Aydan, Ö. 2005. Characteristics and geo-engineering aspects of the 2003 Bingöl (Turkey) earthquake. *Journal of Geodynamics* 40, 334–346.
- USGS (United States Geological Survey). <http://usgs.gov>. June, 2022.
- Utkucu, M., Budakoğlu, E., Çabuk, M. 2018. Teleseismic finite-fault inversion of two Mw = 6.4 earthquakes along the East Anatolian Fault Zone in Turkey: the 1998 Adana and 2003 Bingöl earthquakes. *Arabian Journal of Geoscience* 11, 1–14.
- Utsu, T. 1984. Estimation of parameters for recurrence models of earthquakes. *Bulletin of Earthquake Research Institute* 59, 53–55.
- Wu, C., Shelly, D., Gomberg, J., Peng, Z., Johnson, P. 2013. Long-term changes of earthquake inter-event times and low-frequency earthquake recurrence in central California. *Earth Planetary Science Letters* 368, 144–150.
- Yadav, R., Tripathi, J., Rastogi, B., Das, M., Chopra, 2010. Probabilistic assessment of earthquake recurrence in northeast India and adjoining regions. *Pure Applied Geophysics* 167, 1331–1342.
- Zabcı, C., Akyüz, H. S., Sançar, T. 2017. Palaeoseismic history of the eastern part of the North Anatolian Fault (Erzincan, Turkey): Implications for the seismicity of the Yedisu seismic gap. *Journal of Seismology* 21, 1407–1425.

